Journal of Hydrospace Technology, Vol. 1, No. 2, 1995, pp. 167-186

On the Development of Design Wave Loads in Classification Rules

Jae-Young Song,* Young-Kee Chon, * and
Tae-Bum Ha*

Abstract

In this study, the unified requirements of IACS on longitudinal strength of ships are verified through the nonlinear time domain analyses in irregular waves. The formula for the horizontal shear force, bending moment and torsional moment for ships of large deck openings are proposed based on the calculation results for existing ships. Also, external hydrodynamic sea pressure, accelerations and motions are calculated using linear strip theory and the corresponding design formulae are proposed.

The calculated results are compared with the existing classification rules and will be incorporated into the rules in the near future after more detailed verification.

1 Introduction

The structure of a ship shall survive various loadings imposed on it during her life time and the analytic and computer aided numerical analyses have been employed to confirm its survivability. On the other hand, the structural rules in classification societies have been used as a design guideline for securing ships' structural integrity in addition to their basic purpose of giving minimum design requirements.

In this paper, theoretical investigations of the design wave loads based on the calculations for the existing ships are carried out in the process of the reformation of the rules and the incorporation of modern technological advancement made since last revision. The rules for the hydrodynamic loadings are newly proposed and compared with those of other Societies.

IACS UR S11 is confirmed through the nonlinear time domain analyses in irregular seas. The formula for horizontal shear force, bending moment and torsional moment for the ships of large deck openings are proposed. The lengthwise and depthwise distribution of hydrodynamic pressure as well as motions and accelerations are also proposed based on the calculation results using linear strip theory.

*Member, Korean Register of Shipping

The proposed results were found generally compatible with the current rules of Korean Register of Shipping and those of other classification rules except local hydrodynamic pressure. This difference can be understood when considering the fact that there are so many factors involved in the rules which determine structural scantlings such as allowable stresses of various structural members and there can be conceptual difference in relative emphasis put on global members and local ones, while the theoretical consistancy in the formation of the rules is to be maintained and accuracy of softwares is to be considered.

2 Wave Loadings for Longitudinal Strength

2.1 IACS UR S11

The IACS unified requirement S11 had been established in 1989 owing to the intensive effort of many experts from each member Society since the end of '70s. The nonlinear wave induced bending moment (hereafter, "WIBM") in UR S11 had been determined from the theoretical calculations and full scale measurements after the evaluation of minimum section modulus from the statistics of existing ships and then taking into account of the ratio of WIBM and still water bending moment, for which the details are described in [1, 2].

The expressions for WIBM in IACS UR S11 are as follows.

$$M_w(+) = 0.19MCL^2BC_b \qquad (kN \cdot m) \quad for\ hogging \tag{1}$$

$$M_w(-) = -0.11MCL^2B(C_b + 0.7) \qquad (kN \cdot m) \quad for\ sagging \tag{2}$$

where C means the equivalent static design wave height which gives the long term WIBM at the probability of 10^{-8} and minimum C_b is taken as 0.6. Hereinafter, L, B and d represent the ship length, breadth and summer loaded draft respectively, C_b represents the block coefficient and ρ represents the density of sea water. When $C_b = 0.6$, sagging moment is about 25% larger than hogging moment, which represents the nonlinearity in wave induced loads.

On the other hand, wave induced shear forces(hereinafter, "WISF") in UR S11 are given as

$$F_w(+) = 0.3F_1CLB(C_b + 0.7) \qquad (kN) \tag{3}$$

$$F_w(-) = -0.3F_2CLB(C_b + 0.7) \qquad (kN) \tag{4}$$

the factors M, F_1, F_2 in Equations (1), (2), (3) and (4) denote the longitudinal distribution coefficients of WIBM and WISF given in Ref.[1]

2.2 Calculation of Nonlinear Wave Loads

The nonlinear wave loads are calculated using the software developed in this Society to confirm UR S11, for which its theoretical background is described briefly in the following.

As is well known, the major shortcoming of the linear theory employing linearized free surface boundary condition is that the relative motions of structure and wave are neglected

and geometrical nonlinearity involved in the evaluation of hydrodynamic coefficients in large amplitude waves is excluded.

The method of time domain seakeeping anaysis introduced at the beginning of 1960's by W.E.Cummins[3] follows the instantaneous free surface position on the structure in this respect. With the aids of today's increasing capacity of hardware, practical time domain analyses are now commonly used despite of its complexity.

Extreme cautions and effective numerical methods are needed in the evaluation of impulse response function in the form of convolution integral[4]. In the present analysis, based on the fact that the memory effect due to previous response in convolution integral diminishes within resonably short duration in the practical viewpoint, numerical method employing momentum equation is used despite of the theoretical weakness embedded in the problem. However it can be considered quite resonable in this case since the characteristics of seakeeping equations of motion is dominated by restoring and inertial forces. Accordingly, nonlinear wave loadings in irregular sea are simulated and compared with UR S11.

2.2.1 Equation of Motions and Loads

Under the assumption of potential flow, a vessel is considered to travel with speed U in regular harmonic waves encountering in 180 degree (head sea condition). Then the equation of coupled vertical plane motion η_3(heave) and η_5(pitch) can be written as

$$\sum_i I_{ij} \cdot \eta_j(t) = F_i^T(t), \quad (i = 3,\ 5, j = 3,\ 5) \tag{5}$$

where subscript i, j denote the mode of motion (3:heave, 5:pitch), I_{ij} represents virtual mass plus mass moment of inertia, F_i^T represents the exciting force or moment corresponding to the mode of motion. The wave profile can be written as $\zeta(x,y) = Acos(kx + \omega_e t)$ where A is wave amplitude, k and ω_e represent wave number and encounter circular frequency respectively. With the above, the instantaneous relative vertical displacement $r(x,t)$ at position x(positive forward) from LCG can be written

$$r(x,t) = \eta_3 - x\eta_5 - \zeta(x,t) \tag{6}$$

The relative vertical velocity and acceleration can be expressed as the 1st and 2nd total derivative of Eq.(6) repectively. The right hand side of the Eq.(5) can be decomposed as

$$F_i^T(t) = F_3^m(t) + F_3^D(t) + F_3^R(t) \tag{7}$$

where superscript m denotes the force due to fluid momentum change caused by ship motion, D means the force due to diffraction of incoming wave and wave making damping and R means the dynamic estoring force of which their expressions are shown below.

$$F_3^m(t) = -\int_L a_{33}(x,t)\frac{D^2 r}{Dt^2}dx - \int_L \frac{Da_{33}(x,t)}{Dt}\frac{Dr}{Dt}dx \tag{8}$$

$$F_3^D(t) = -\int_L [b_{33}(x,t)\frac{Dr}{Dt}|dx \tag{9}$$

$$F_3^R(t) = -\int_L \rho g[\int_{c'(x)} zdy - \int_{c(x)} zdy]dx \tag{10}$$

where $a_{33}(x,t)$ and $b_{33}(x,t)$ represent the added mass and damping coefficient of a section respectively corresponding to vertical relative position of the section, $C'(x)$ and $C(x)$ in Eq.(10) represent the hull contour below waterline at certain time t and static equilibrium condition respectively. The first term of right hand side of Eq.(8) is the added mass force proportional to vertical relative acceleration. The 2nd term is the force due to the rate of change of fluid momentum of timely varying sectional added mass. Since the time gradient of added mass Da_{33}/Dt is directly related to the sectional draft change in time, this value will vary when there is a great geometrical depthwise change at a section. In this respect, this force is often called as flare force[5].

The substituion of Eq.(6)-(10) to Eq.(5) leads to the equation of coupled vertical plane motion in time domain. In order to solve this Equation, Newmark- β method is employed. For the equation of pitch motion, each force term in the integrand of Eq.(8)-(10) is multiplied by the moment arm x which is the distance of corresponding section from LCG. The hydro-elastic problem can also be treated in this way in conjuction with beam deflection equation, however, they are omitted in this paper.

In Fig.1 and 2, the time history of midship WIBMs and WISFs at station 17 are shown respectively for two ships of $C_b = 0.581$ and $C_b = 0.845$ in regular harmonic wave(The station No.1 means A.P. and No.21 means F.P. in this paper), in which transient initial responses are discarded. As can be anticipated, the nonlinearities increase as C_b becomes smaller due to nonlinear buoyancy force caused by the fact that full after body of the ship relatively larger than bow portion is submerged in hogging condition. On the other hand, the periodic irregularities in the Figures are the effect of flare force which is showed up at the time of negative relative vertical velocity when the bow portion of the ship immerses. At the time of bow immersion of the ship, the value of a_{33} is taken as that of infinite frequency in this calculation[5]. The above nonlinearities in wave loads are affected greatly by the wave height. The ratio of sagging to hogging WIBM according to C_b are shown in Fig.3, which shows larger nonlinear effect in small C_b ship as wave height increases.

It is to be noted that for $C_b = 0.84$ sagging to hogging WIBM ratio is about 0.95 while IACS UR S11 gives the corresponding ratio of 1.06. Although this can be varied according to the frequency of incoming wave, the same result is shown in Ref.[7]. It turns out to be that the sagging moment is larger than hogging moment in the analyses for irregular sea as is described in the following section.

2.2.2 Wave Loads in Irregular Sea

To expand the above results for irregular sea, irregular wave is generated using ITTC spectrum for given $H_{1/3}$ and average period. From the definition of the spectrum, the wave amplitude can be written as

$$A(\omega_{oi}) = \sqrt{2S(\omega_{oi}) \cdot \Delta\omega_{oi}} \tag{11}$$

Then, the surface profile of irregular sea is given as

$$\zeta(x,t) = \sum_{i=1}^{N} A(\omega_{oi})(k_i x + \omega_{ei} t - \varepsilon_i) \tag{12}$$

The total 90 component waves are taken in the present calculations. The example of irregular wave time history is shown in Fig.4. The time history of response in irregular sea shown in Fig. 5, 6, 7 and 8 can be obtained through the linear sum of steady responses for each component regular wave (say, Fig. 1, 2) calculated as described in 2.2.1 taking account of random phase diffenrences. The simulations of the response are carried out for each component wave for 50 minutes and only steady responses are taken to superimpose them linearly. The time history of WIBM and WISF of the ship of $C_b = 0.581$ for the irregular wave(Fig.2) of $H_{1/3}$, $T_1 = 11.62$ sec. are shown in Fig.5 and 6 respectively and for the ship of $C_b = 0.845$ in Fig.7 and 8. Comparing Fig.5 with Fig.6, the tendency of great sagging moment is also shown and it becomes more clear in the case of the small C_b ship. Many peaks in Fig.5 are come from the flare force effect.

2.2.3 Statistical Analyses and Verification of the Rule

For the verification of the rules incoporating the foregoing nonlinear wave loads, long term statistical analyses considering ships life time are needed. However the amount of calculation involved in this work is enormous so that only standard deviations of short term response are calculated to confirm UR S11. The standard deviations are obtained directly from the time history by counting the positive peak(hogging) and negative one(sagging). The standard deviations at each section can be written as

$$\sigma(-) = \sqrt{\frac{\sum M_-^2(t)}{N}}, \quad \sigma(+) = \sqrt{\frac{\sum M_+^2(t)}{N}} \tag{13}$$

where M_+, M_- denote the hogging or sagging bending moment respectively, N is the number of peaks in response time history, The ratio of longitudinal distribution of standard deviations of WIBM and WISF nondimensionalized by midship sagging moment and shear force at St.17 respectively are illustrated in Fig. 9 - 12 for comparison. The results of present calculation, UR S11 and those of Ref.[7] comply with satisfiable accuracy.

2.3 Torsional Moment for Ships of Large Deck Opening

2.3.1 Investigation of Current Rule

It is well known that, in the case of ships of large deck opening such as containers and bulk carriers, the warping stress induced by the torsional moment is one of the important hull girder stresses. It is to be combined with those due to horizontal, vertical WIBM and still water bending moment. In Ref.[9], the warping stress σ_W is calculated by assuming the lengthwise distribution of WITM be the form of cosine funciton, and combine the total hull girder stress as

$$\sigma_T = \sigma_S + \sqrt{(0.75\sigma_V)^2 + \sigma_H^2 + \sigma_W^2} \tag{14}$$

In above, σ_S, σ_V and σ_H denote stress due to still water bending moment, vertical WIBM and horizontal WIBM respectively. However the distribution form of cosine function for WITM is not practically resonable when considering the difference in the longitudinal distribution between long term WITM and WITM due to single design wave. Further, the critical longitudinal position is to be considered in view of torsional moment. On the other hand, the phase differences are neglected between each component of stresses in Eq.(14), which yield overestimation of σ_T.

2.3.2 Formation of the Rule for WITM

In view of above consideration, it is needed to look into the components consisting WITM. The sectional torque with reference to shear center can be devided into two groups as the roll moment at origin of the section denoted by M_{T_2} and the moment due to the sectional horizontal force multiplied by the arm between sectional origin and shear center denoted by M_{T_1}. Then sectional torque can be written as

$$M_T = M_{T_1} \pm M_{T_2} \tag{15}$$

where double sign in Eq.(15) is introduced to take maximum case of M_T due to phase difference of M_{T_1} and M_{T_2}. From the definition of M_{T_1}, it can be approximately written as

$$M_{T_1} = Q_H(x) \cdot (d + S_C) \tag{16}$$

where $Q_H(x)$ denotes the horizontal sectional shear force, S_C is the distance from keel to shear center(positive downward). From Eq.(16), it follows that the distribution of M_{T_1} depends on that of $Q_H(x)$. Since most of the cargo ships have after-engine room, the torsional moment is sustained by the engine room front bulkhead which is located about L/4 from A.P. Thus, it is quite reasonable that the design basis is considered at L/4 station. On the other hand, for any of the stations in question, calculated equivalent wave system based on long term torsional moment is comparable to that derived from long term lateral bending moment. When the vessel is operating in a seaway, both maximum torsional moment and maximum lateral bending moment would occur in approximately the same instant, therefore producing a most critical condition of lateral loading. Therefore, it is possible to define one equivalent design wave system which would yield both the maximum torsion and the maximum lateral bending moment at the specific station to generate load information for investigating structural response in the lateral plane.

In this study, the design wave is based on the long term lateral WIBM at midship, of which the wave to ship length ratio (λ/L) is normally about 0.5 and wave to ship heading angle is 60 or 120 degree. This approximately corresponds to design wave based on horizontal WISF at L/4 station, for which their typical distribution is shown in Fig.13. Further, the phase difference between $Q_H(x)$ at L/4 station and incoming wave is approximately $\pi/2$, $Q_H(x)$ is domainated by the imaginary part as can be shown in Fig.13. With the above, the distribution of imaginary part of $Q_H(x)$ in Fig.13 is approximated by sine curve

and linear regression was carried out for the magnitudes at L/4 station for 17 exsting ships as shown in Fig.14, which yields

$$Q_H(x) = 0.56CLd(C_b + 0.7) \cdot sin\frac{2\pi x}{L} \tag{17}$$

Intergrating above Eq.(17) from A.P. to midship gives the horizontal wave bending moment at midship section as

$$M_{WH} = \int_0^{L/2} Q_H(x)dx = 0.18CL^2d(C_b + 0.7) \tag{18}$$

of which the results are shown in Fig.15. The present result lies between current KR and GL rule.

For M_{T_2}, the typical distribution is shown in Fig.14 which is the imaginary part of torsion moment based on the same design wave as M_{T_1}. This distribution is approximated as constant value along ship length and maximum magnitude is taken in this formation. Although it is far from the theoretical basis and causes unbalance moment at fore and after end of a ship, since torsional rigidity is focused at the engine room forward bulkhead and forepeak bulkhead, it would not have significant meaning in practical sense.

The calculated results for existing ships and their regression results are shown in Fig.17, which yield

$$M_{T_2} = 0.039CLB^2 \tag{19}$$

Finally, the torsional moment can be written as

$$M_T = M_{T_1} \pm M_{T_2} = 0.56CLd(C_b + 0.7)sin\frac{2\pi x}{L}(d + S_C) \pm 0.039CLB^2 \tag{20}$$

2.3.3 Combination of Stresses

The combination method of square root sum such as in Eq.(14) is not needed any more once M_{WH} and M_T are evaluated with the same design wave as in the foregoing. It can be put together linearly except σ_V. To get rid of this problem, the ratio of long term vertical bending moment to vertical bending moment due to the design wave used in evaluating M_{WH} or M_T is analysed and they can be approximated as 0.5, which gives the final expression of combined stress as

$$\sigma_T = \sigma_S + 0.5\sigma_V + \sigma_H + \sigma_W \tag{21}$$

3 Hydrodynamic Pressures Acting on Outer Shell

Besides hull girder wave loads discussed above, the structural members are under local hydrodynamic pressure which deviates from each other Classification Rule . This results from the conceptual differences in dealing with the local hydrodynamic pressure. Mostly,

is also decided from the characteristic shape parameters and their approximated values from [13]. Finally,

$$T_\theta = 2\pi(\frac{I_{\theta\theta} + A_{\theta\theta}}{C_{\theta\theta}})^{1/2} \cong 1.86\sqrt{L/g} \quad (sec) \tag{29}$$

where $I_{\theta\theta}$, $A_{\theta\theta}$, $C_{\theta\theta}$ represent inertia moment, added inertia and restoring moment respectively. From Eqs. (28) and (29), the design acceleration due to pitching motion can be written as

$$a_\theta = \theta \cdot (\frac{2\pi}{T_\theta})^2 \cdot l_\theta \qquad (m/sec^2) \tag{30}$$

where l_θ is the distance from LCG to the point considered.

4.2 Lateral Plane Motions and Accelerations

As for the case of pitch motion, the speed effect on sway and yaw is found negligible, so that the linear regression analyses for the sway and yaw accelerations based on $1/L$ result in following two equations.

$$a_y = 178/L + 0.36 \qquad (m/sec^2) \ \ for\ sway \tag{31}$$

$$a_\psi = (6.95/L - 0.017) \cdot l_\psi \quad (m/sec^2) \ \ for\ yaw \tag{32}$$

where l_ψ is the distance from LCG to the point considered. In Fig.27 and 28, the result of calculation for various ship speed and their regression analyses are shown.

4.3 Roll motions and Accelerations

It is well known that the viscous damping effect in roll motion should be considered as well as wave making damping. The practical method based on the experiments is used such as in [14]. On the other hand, the roll motion amplitude is represented in terms of C_b, L, B, d and some other characteristic parameters of the ship in IMO Res.A562[15]. In this paper, foregoing parameters are further simplified based on the statistics of existing ships.

Finally, the period and amplitude of roll can be given as

$$T_\phi = \frac{2C_f \cdot B}{\sqrt{GM_T}} \qquad (sec) \tag{33}$$

$$\phi = k \cdot C_S \cdot f \cdot \sqrt{0.131 - 0.005T_\phi} \quad (rad) \tag{34}$$

Therefore, the design acceleration due to roll motion can be written as

$$a_\phi = \phi \cdot (\frac{2\pi}{T_\phi})^2 \cdot l_\phi \qquad (m/sec^2) \tag{35}$$

where, $C_f = 0.373 + 0.023(B/d) - 0.043(L/100)$

For the ship of small C_b, loadline point pressure increases rapidly at the forward part of the ship while it is not in the after part. And C_b over 0.85 does not affect K_1 value at the forward part, so that the maximum value of C_b is taken as 0.85. Having the local hydrodynamic sea pressure below the loaded waterline as in Eq.(23), the pressure above the loaded waterline is determined under the assumption that the waterline pressure, P_f in Eq.(22), linearly varies with the height from the waterline. The maximum dynamic wave rise is taken as the pressure head equivalent to the long term pressure of 10^{-8} probability level at the waterline as shown in Fig.22.

This comes from the realization that the pressure above the sea level could be reasonably decided by considering the most probable values she may experience during her lifetime. Thus, the long term pressure at loaded waterline of 10^{-8} probability level is derived from the linear regression analyses for the 17 existing ships as

$$P_u = 0.098L + 83.7 \qquad (kN/m^2) \tag{25}$$

which yields the final expression for the hydrodynamic sea pressure above loaded waterline as

$$P = P_f \cdot K_1(1 - 10h/P_u) \qquad (kN/m^2) \tag{26}$$

where K_1 is the longitudinal distribution factor in Eq.(23), h is the vertical distance from loaded waterline. The results of comparison with DnV rules are shown in Fig. 23, in which the correlation is good for large h, i.e, large freeboard. In Fig. 24, the upper deck sea pressures are compared for varying ship length, where the correlation becomes better for large ship length.

4 Motions and Accelerations

4.1 Vertical plane motions and Accelerations

In Fig. 25, the long term vertical accelerations at LCG of 10^{-8} probability level are shown for varying ship length and speed, where the speed effect becomes smaller as the ship length increases. Taking account of these fact and linear regression analyses based on $1/L$ and $1/\sqrt{L}$ yield following vertical accelerations as,

$$a_z = \frac{V^{1.2}}{2\sqrt{L}} + \frac{361}{L} + 0.49 \qquad (m/sec^2) \tag{27}$$

of which the results are shown in Fig.25 as solid line. On the other hand, based on the analyses that the speed effect on pitching motions is negligible, the formula for pitching motion can be written as

$$\theta = \frac{19.62}{L} + 0.022 \qquad (rad) \tag{28}$$

which is based on the analyses when Fr. No.=0.1. Eq.(28) yields larger motions by about 30% than those of [12] as shown in Fig.26. The formula for natural period of pitch motion

the local pressure is evaluated through the long term analyses of the hydrodynamic pressure at the concerned position with certain probability level, say 10^{-8}. However, this has basic shortcomings neglecting the fact that long term pressures at each point on the shell do not occur at the same time. Thus, local long term pressure at 10^{-4} probability level seems resonable compromise which corresponds to traditional deterministic method.

Fig.18 excerpted from Ref.[11] presented by Prof. H. Soeding clearly shows the discrepancies of local pressures of different probability levels, which are independent of hull girder loads.

In the present formation, local hydrodynamic pressure is calculated using the design wave based on the hull girder vertical bending moment which is different from the above mentioned method calculating local long term pressure itself.

In Fig.19 the calculated hydrodynamic pressure head at the loadline point of midship section is illustrated for varying ships length together with their regression result and those of current DnV rule and KR rule. It is interesting to know the fact that the present value, evaluated using the design wave based on the 10^{-8} probability level of long term vertical WIBM, is approximately half of the value based on the 10^{-8} probability level of long term pressure of local point(current rule). Thus the traditional deterministic method taking the local pressure head as the half of that of global load can be justified. Moreover, the results of present calculations are almost the same as DnV's tentative rule value which is defined as the local long term pressure of 10^{-4} probability level.

Finally, the regression analyses for the present local pressure for the midship loadline point yields

$$P_f = 0.095L + 33.4 \qquad (kN/m^2) \tag{22}$$

It is worthwhile to note that the local stress due to above pressure can be directly combined with the global longitudinal stress due to global vertical bending moment since the same design wave is employed owing to no phase difference between them.

Above pressure acting on the loadline point of midship section varies lengthwise as well as depthwise as shown in Fig.20 and Fig.21. In Fig.20, lengthwise variation of the ratio of pressure at bilge point to that of loadline is shown, i.e., depthwise variation of pressure in longitudinal location of ships. The lengthwise variation of pressure at loadline point is shown in Fig.21. Using the results contained in Fig.20 and 21, the hydrodynamic pressure on the outer shell below loaded waterline is proposed as

$$P_T(x, y, z) = P_f \cdot K_1 \cdot (1 - \frac{K_2 h}{d}) \tag{23}$$

where $K_1 = 1.0$ for $0.4L$ midship, $K_1 = 1.5$ for after portion of A.P. . For forward part from F.P., K_1 is defined as

$$K_1 = \frac{5.5(0.85 - C_b)}{1 - C_b^2} + 2.0 \tag{24}$$

while $K_2 = 0.5$ for $0.4L$ midship and 0.1 for forward part from F.P and after part from A.P.. The values of K_1 and K_2 for the rest of the longitudinal locations are taken linearly interpolated.

GM_T = transverse metacentric height

= $0.12B$ for tanker and bulk carrier

= $0.07B$ for other ships

C_S = 0.82 for tanker and bulk carrier

= 0.96 for other ships

$$f = 0.86 + 2.72C_b - (B/d)(0.11 + 0.34C_b)$$

and l_ϕ is the distance from the center of rotation to the point considered and can be taken as the lesser of $(D/4 + d/2)$ and $(D/2)$ from the baseline. In above equations T_ϕ, C_b and (B/d) are limitted as

$$6.0 \leq T_\phi \leq 20.0, \quad 0.45 \leq C_b \leq 0.7, \quad 2.4 \leq (B/d) \leq 3.5 \tag{36}$$

The results of Eq.(34) is compared with other rules together with the calculations for 17 existing ships as shown in Fig.29. The calculated results are far below the rules and the present results of Eq.(34) fall in-between the other rules.

5 Conclusions

Almost all the wave loading components which formulate the bases of classification rules are investigated and the new formulae are proposed through the extensive calculations for existing ships in this paper. IACS UR S11 is confirmed using nonlinear time domain analyses. For the ships with of large deck openings, consistent analyses for horizontal force, benging moments and torsional moments were carried out and the stress combination method is newly proposed.

The rules for hydrodynamic external sea pressure are proposed based on the design wave which gives the long term vertical wave bending moment of 10^{-8} probability level, which are compatible with other classification rules and enables the linear combination of global and local stress directly. Also, the formulae for motions and acceleration are proposed. The above results will finally be incorporated in the structural rules after more detailed verification in the near future.

References

[1] K.R, "Amendment of Rules for Classification of Steel Ships,"*Korean Register of Shipping*, 1989

[2] A.Nitta, H.Arai and A.Magaino, "Basis of IACS Unified Longitudinal Strength Standard,"*Marine Structures*, Vol.5, 1992

[3] W.E.Cummins, "The Impulse Response Function and Ship Motions,"*Schiffstechnick*, Vol.47, 1962

[4] T. Ikebuchi, "Hydrodynamic Force on a Body Moving Arbitrary in Time on Free Surface,"*J.of Kansai Soc. of N.A.Japan*, No.181, June, 1981

[5] R. Borrsen and F. Tellsgard, "Time History Simulation of Vertical Motion and Loads on Ships in Regular Head Waves of Large Amplitude,"*Norweigian Maritime Research*, 1980

[6] Y. Yamamoto, M Fujino and T Fukusawa, "Longitudinal Strength of Ships in Rough Seas,"*NK Bulletine*, 1983

[7] H. Ohtsubo and T. Kuroiwa, "Non-linearity in Sagging Moment and Shear Force of Fine Ships,"*NK Bulletin*, 1989

[8] ABS, "Final Reports on Wave Response Calculation for IACS SHIP,"*ABS Ocean Eng.Dept.Technical Report OED-83014*, Aug. 1983

[9] K.R., "Guidance Relating to Rules for Classification of Steel Ships,"*Korean Register of Shipping*, 1992

[10] G.L., "Rules for Classification and Construction,"*Germanisher Lloyd*, 1992 Ed.

[11] H. Soeding, "Discussion on the Report of Committee 1.2,"*Proc. of 11th ISSC, Elsevier Applied Science*, Vol.3, 1991

[12] B.V., "Rules for Ships, Hull structure Part II-A,"*Bureau Veritas*, 1990

[13] E. V. Lewis, "Principles of Naval Architectures,"*SNAME*,2nd Rev., 1987

[14] Y. Himeno, "Prediction of Ship Roll Damping-State of the Art,"*Univ. of Michigan*, Report No.239, 1981

[15] IMO, "Resolutions of SOLAS Convention,"*Korean Register of Shipping*, 1987

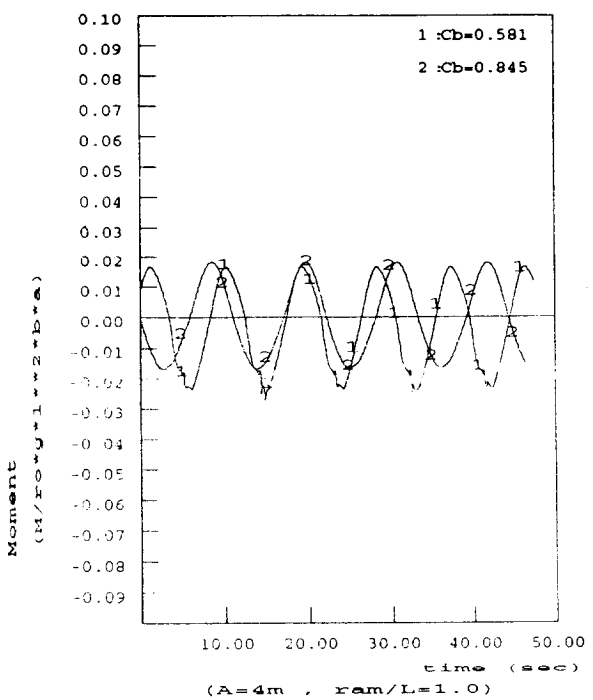

Figure 1: Nonlinear. WIBM at Midship under Regular Wave($F_n = 0.1$)

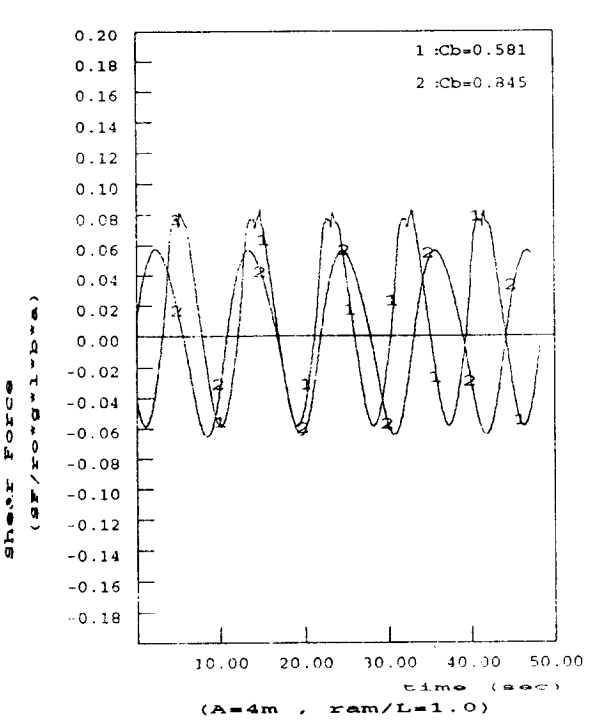

Figure 2: Nonlinear. WISF at 17 st. under Regular Wave($F_n = 0.1$)

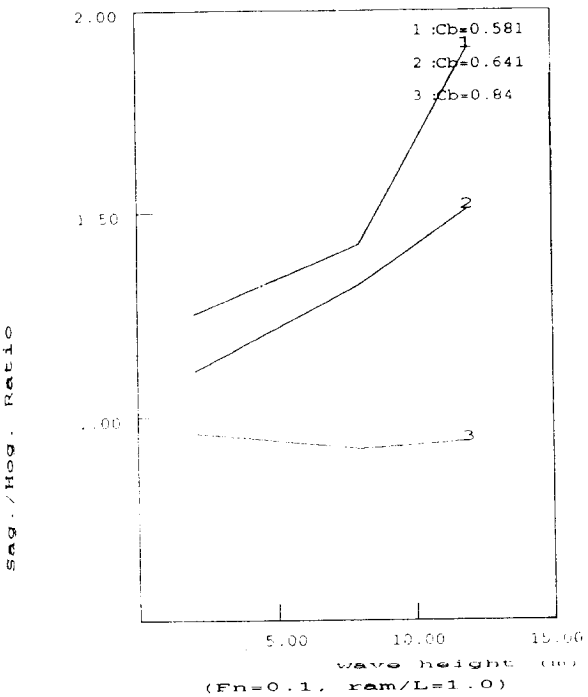

Figure 3: Sag./Hog. Ratio Variation under Regular Wave

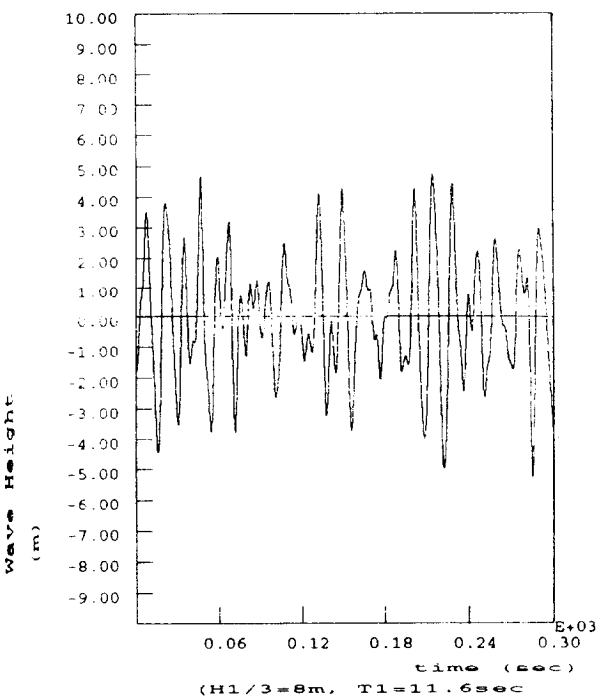

Figure 4: Exam. of Irrg. Wave Generated from ITTC Spectrum

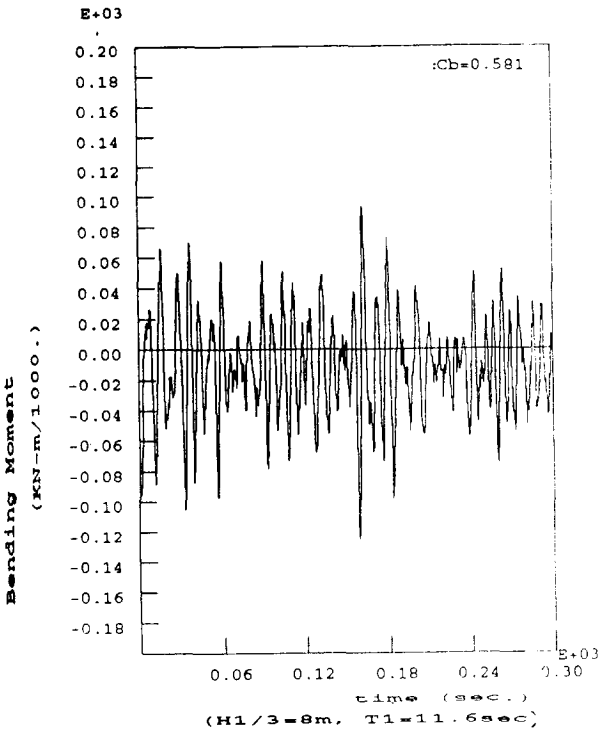

Figure 5: WIBM at Midship induced by irregular Wave($F_n = 0.237$)

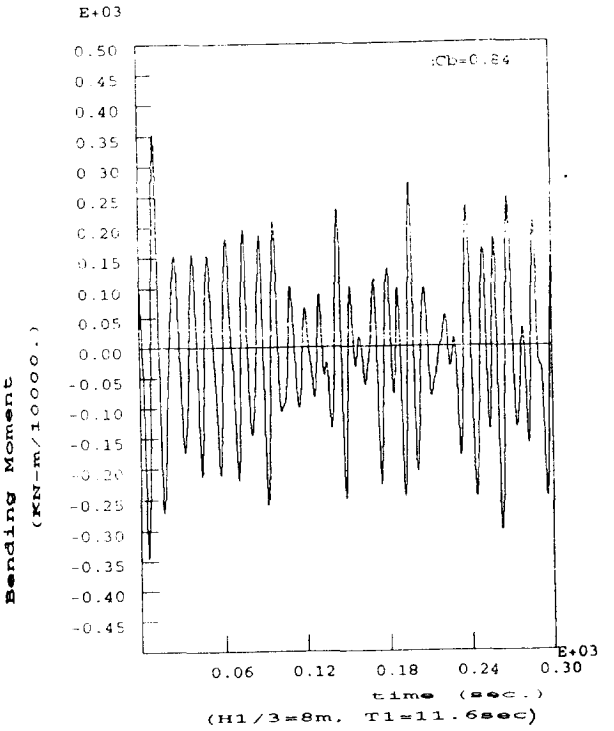

Figure 7: WIBM at Midship induced by irregular Wave($F_n = 0.1$)

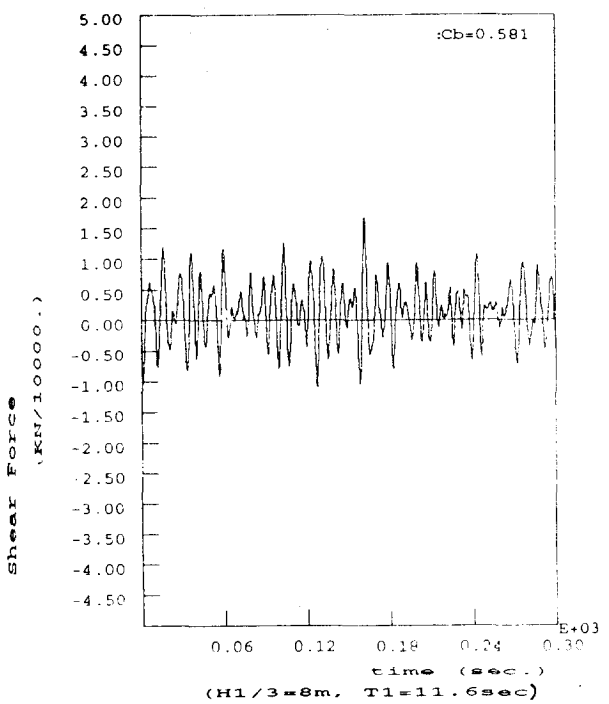

Figure 6: WISF at st. 17 induced by irregular Wave($F_n = 0.237$)

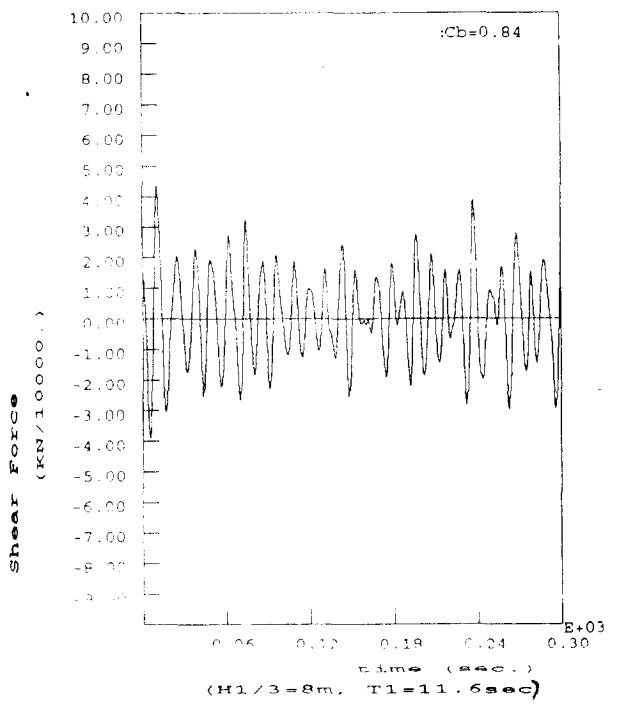

Figure 8: WISF at St. 17 induced by irregular Wave($F_n = 0.1$)

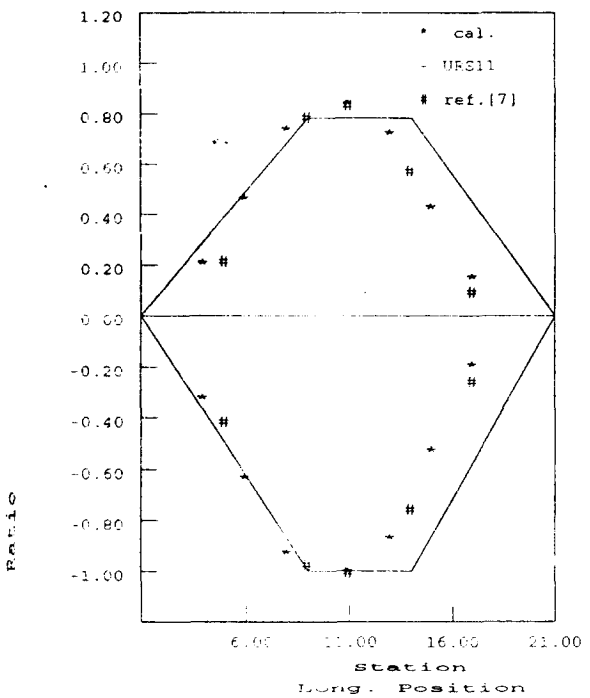

Figure 9: Comp. betw. URS 11 and Cal. for WIBM($C_b = 0.581, F_n = 0.237$) under Irr. Wave($H_{1/3} = 8m, T_1 = 11.6sec$)

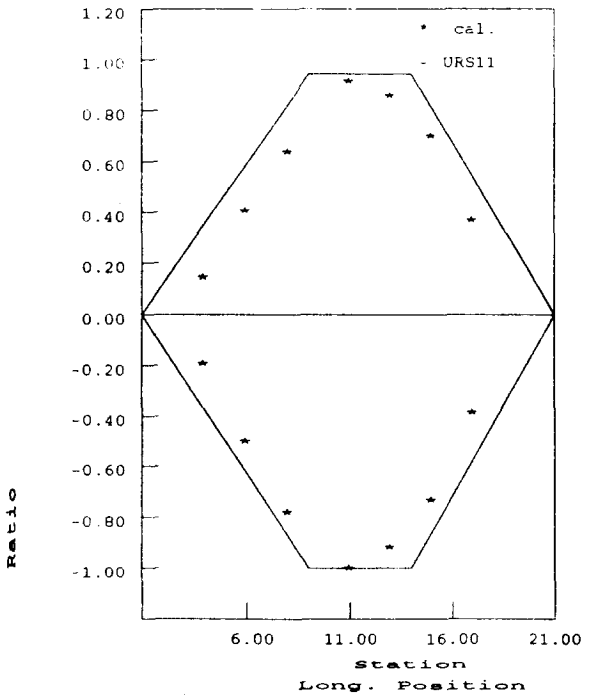

Figure 11: Comp. betw. URS 11 and Cal. for WIBM($C_b = 0.84, F_n = 0.1$) under Irr. Wave($H_{1/3} = 8m, T_1 = 11.6sec$)

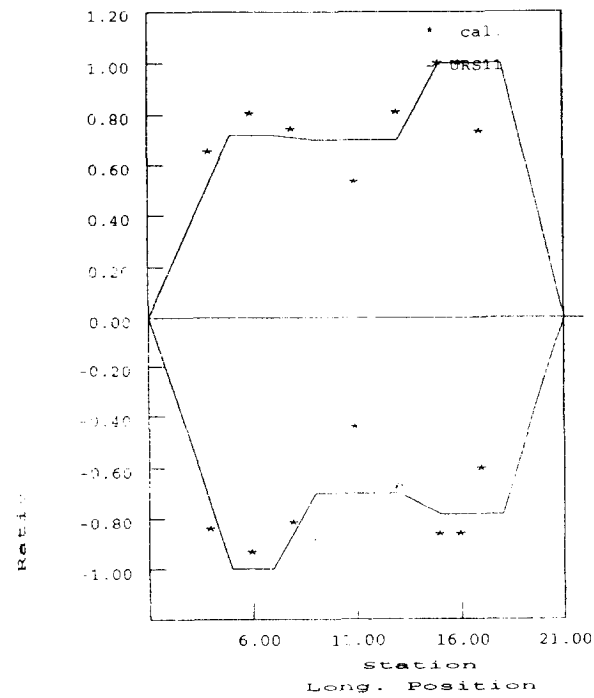

Figure 10: Comp. betw. URS 11 and Cal. for WISF($C_b = 0.581, F_n = 0.237$) under Irr. Wave($H_{1/3} = 8m, T_1 = 11.6sec$)

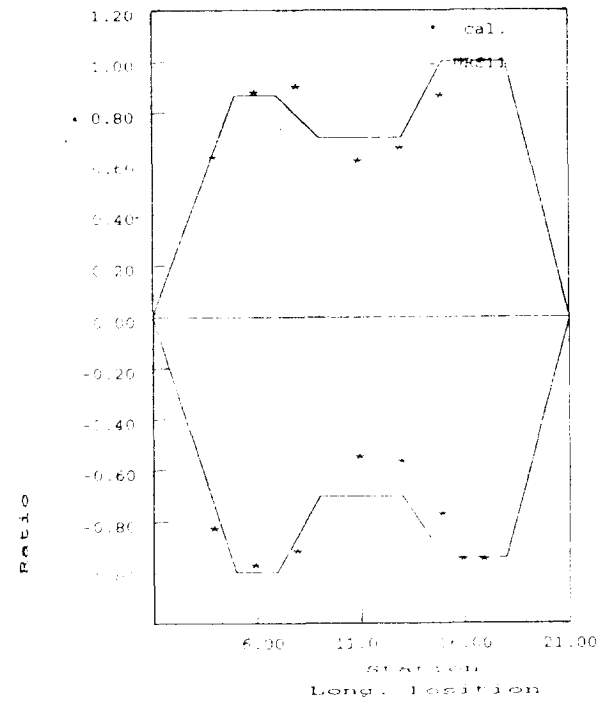

Figure 12: Comp. betw. URS 11 and Cal. for WISF($C_b = 0.84, F_n = 0.1$) under Irr. Wave($H_{1/3} = 8m, T_1 = 11.6sec$)

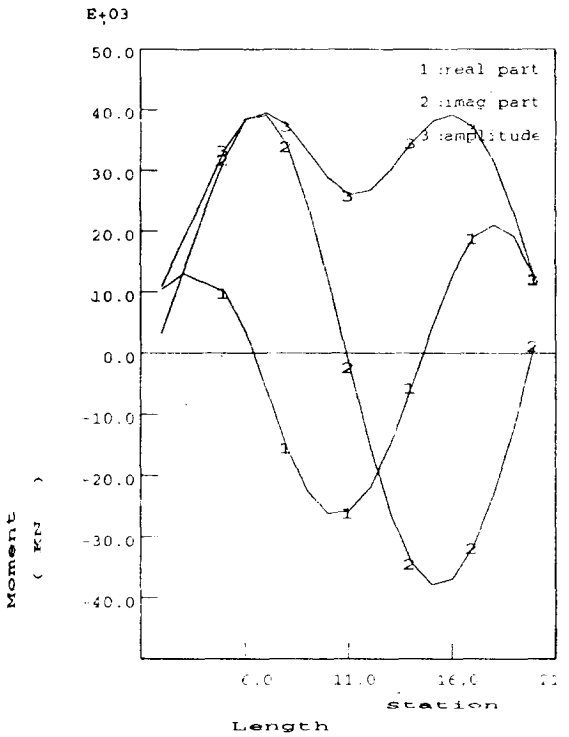

Figure 13: Hor. WISF Distribution along Ship Length for Exam. Ship

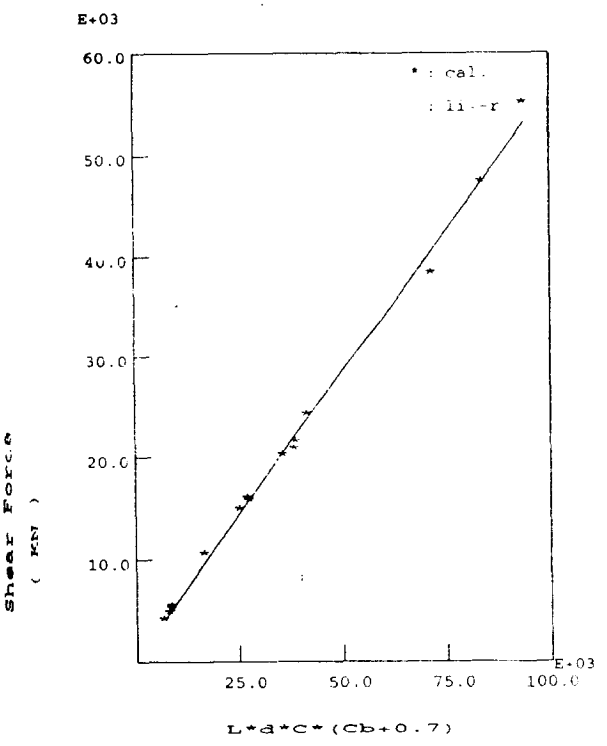

Figure 14: Regression Result of Hor. Shear Force($F_n = 0.1$)

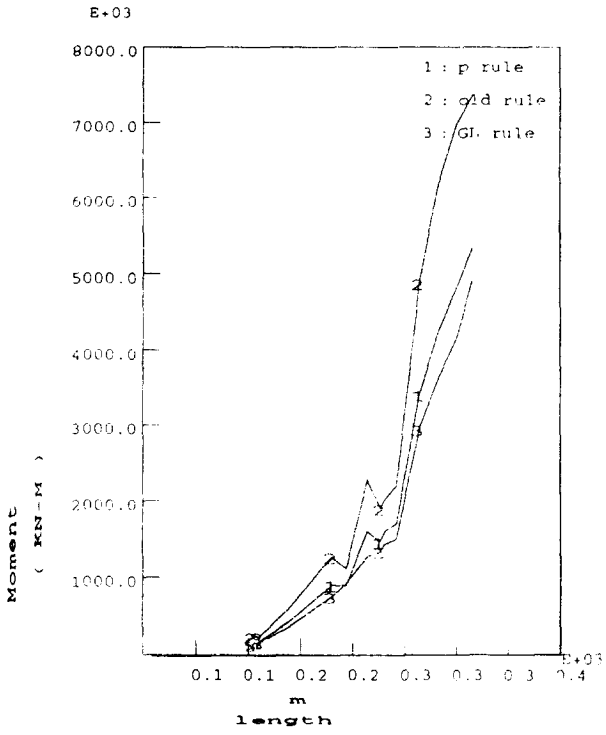

Figure 15: Comp. of Horizontal WIBM

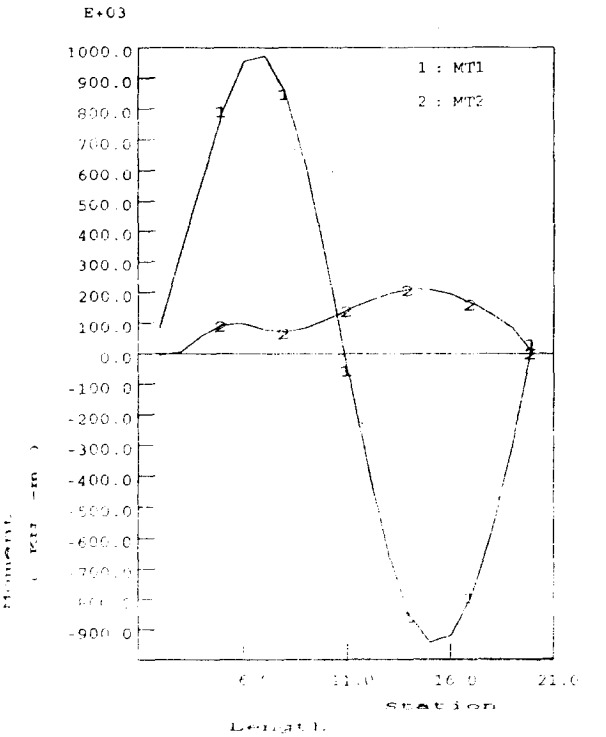

Figure 16: Torsional Mt. Dist. along Ship Length for Exam. Ship

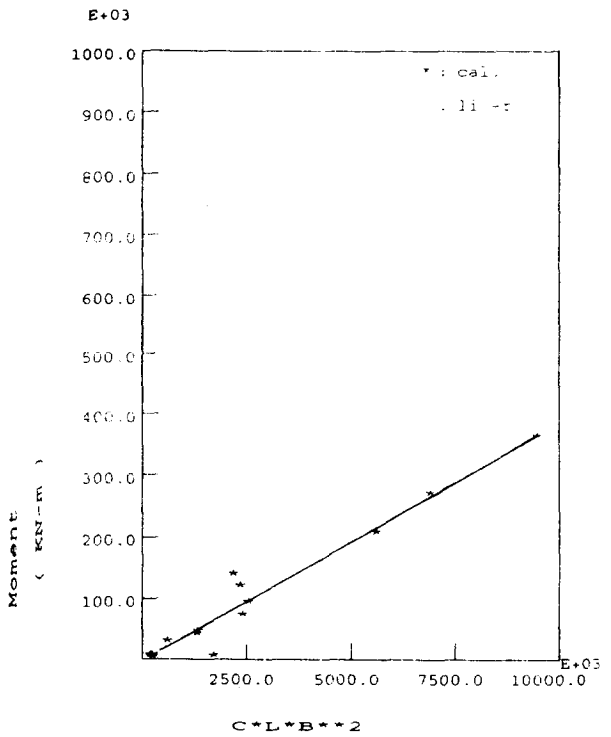

Figure 17: Regression Result of Mt2 ($F_n = 0.1$)

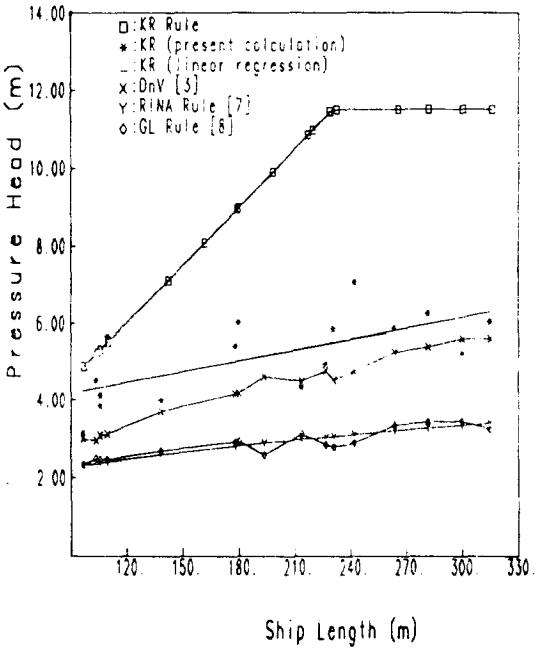

Figure 19: Pressure Versus Ship Length ($F_n = 0.1$)

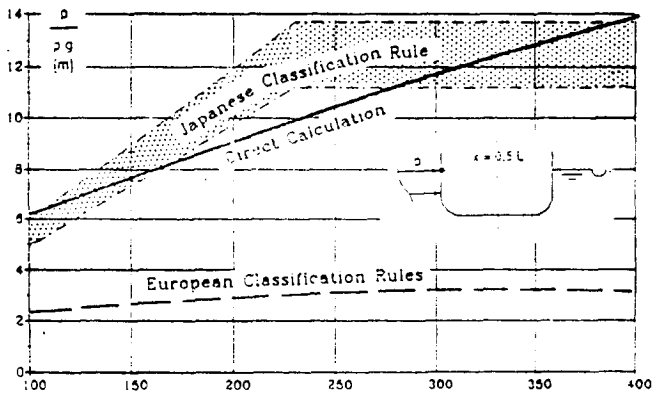

Figure 18: Design Wave Pressure Head on Side Shell at Midship Section as Function of Ship Length(exerpted from Ref[11])

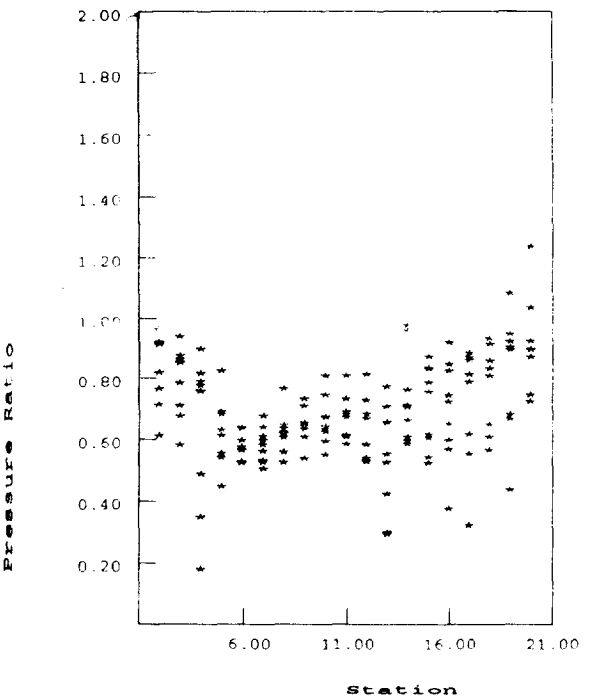

Figure 20: Pressure Ratio betw. Bilge Pt./Free Surface Pt.

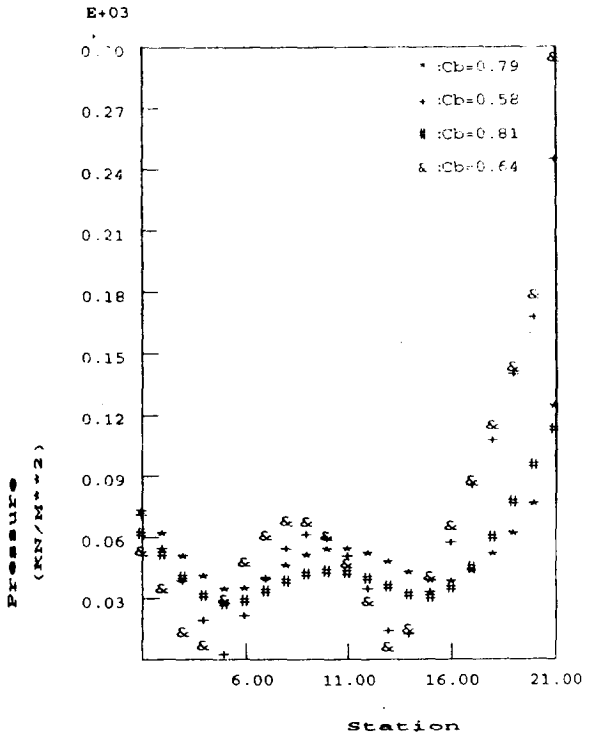

Figure 21: Free Surface Pressure Variation ($F_n = 0.1$)

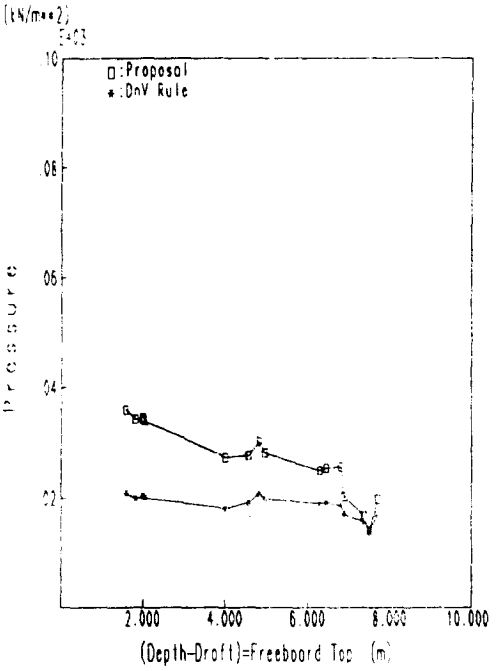

Figure 23: The Comparison of the Pressure of the Freeboard Top

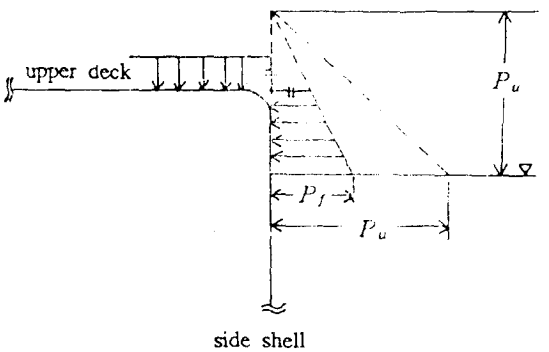

Figure 22: The Pressure acting on Upper Deck and Side Shell above Waterline

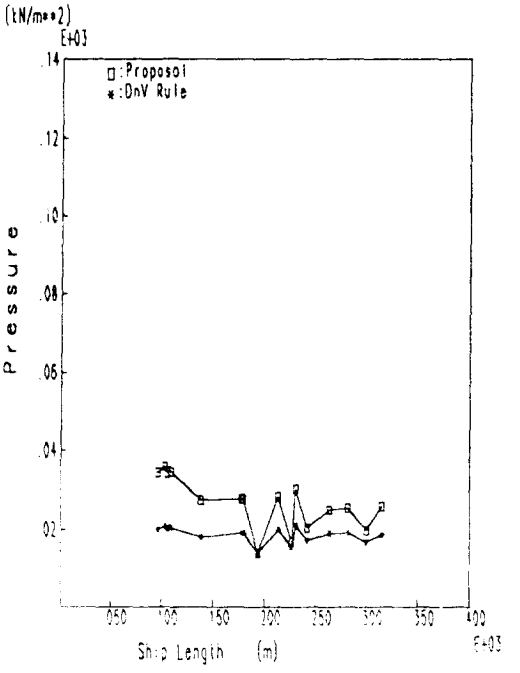

Figure 24: Pressure vs. Ship Length

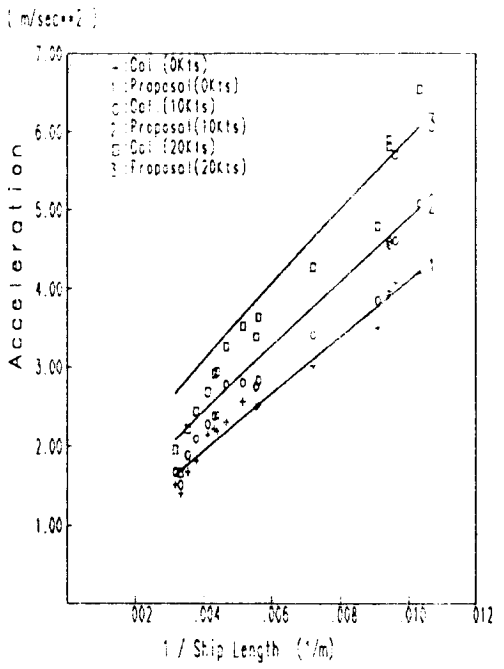

Figure 25: Heave acceleration

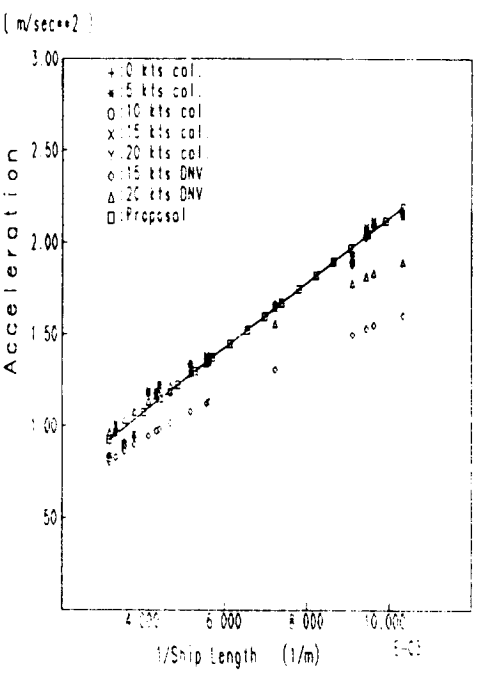

Figure 27: Sway acceleration

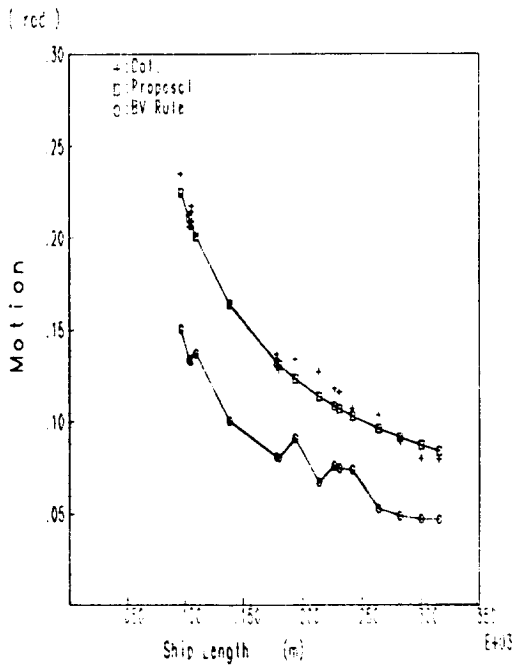

Figure 26: Pitch motion

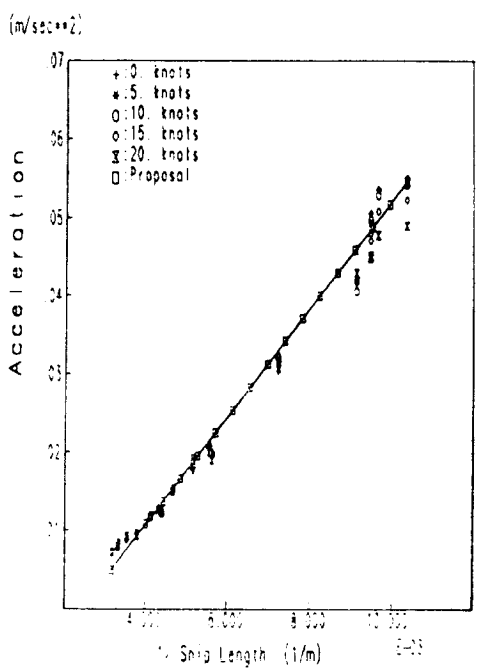

Figure 28: Yaw acceleration

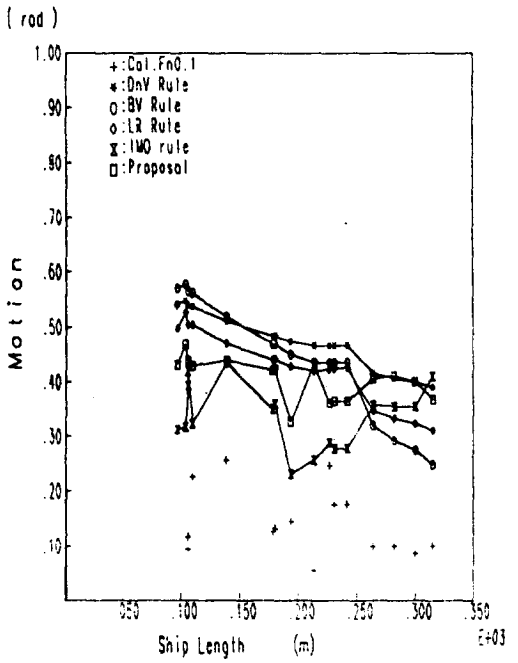

Figure 29: Roll motion